



Optimal LQR Controller Methods for Double Inverted Pendulum System on a Cart

Tayfun ABUT^{1*}

¹ Muş Alparslan University, Mechanical Engineering Department, tayfunabut@gmail.com, Orcid No: 0000-0003-4646-3345

ARTICLE INFO

Article history:

Received 20 February 2023
Received in revised form 7 April 2023
Accepted 1 June 2023
Available online 20 June 2023

Keywords:

Double Inverted Pendulum System on a Cart (DIPSC), Optimal Control, Linear Quadratic Regulator (LQR), GA, PSO, GWO

Doi: 10.24012/dumf.1253331

* Corresponding author

ABSTRACT

Most of the systems in our lives are inherently nonlinear and unstable. In control problems in the field of engineering, the aim is to define the control laws that maximize the operating efficiency of these systems under diverse security coefficients, and constraints and minimize error rates. This study aimed to model and optimally control a Double-Inverted Pendulum System on a Cart (DIPSC). A DIPSC was modeled using the Lagrange-Euler method, and classical and optimal Linear Quadratic Regulator (LQR) control methods were designed for the control of the system. The purpose of the designed controllers is to keep the arms of the double inverted pendulum on the moving cart vertically in balance and to bring the cart to the determined balance position. The critically important Q and R parameters of the LQR control technique that is one of the optimal control techniques were obtained using the Genetic Algorithm (GA), Particle Swarm Optimization (PSO), and Grey Wolf Optimization (GWO) algorithms. The DIPSC system was checked using classical LQR and optimal LQR methods. All obtained results are given graphically. The proposed methods are presented and analyzed in tabular form using Settling time and Mean-Square-Error (MSE) performance criteria.

Introduction

A pair of inverted pendulum systems on a cart is one of the systems that have been tested and validated by the methods proposed in control studies due to their incompletely driven and non-linear structure. The usage areas of these systems are quite wide, from human walking to satellite and rocket modeling, from aircraft landing and take-off to ship balancing modeling, etc.[1-5]. The double-inverted pendulum is based on the principle of balancing the arms with the movement of the cart. This balancing problem is quite difficult since it is driven by a single motor, and the continuous movement of the arms leads to the instability of the system.

In the literature, double-inverted pendulum systems on a cart (DIPSC) have been tried to be controlled by using different control types at different times. Furuta et al., [6] performed the control of a double inverted pendulum on a cart (DIPSC) system in a simulation and experimental environment with a computer program called CADOS. Ceheng et al., [7] performed the control of a real-time DIPSC system obtained by combining composition coefficient fuzzy control theory with LQR optimal control theory. The method was tested on a DIPSC system with a sampling interval of 4 ms. Zhong and Rock [8] proposed a method of energy and passivity-based control of a DIPSCs

system. It has been demonstrated in simulation studies that it can stabilize the system steadily from any initial position. Bogdanov [9] proposed and simulated controller approaches for optimal control of a DIPSC system, consisting of LQR, situational Riccati equation, optimal neural network control, and their combinations. The simulations revealed the superior performance of the controller designed with the situational Riccati Equation over LQR and the improvements provided by the neural networks that compensate for the model deficiencies in LQR. Cheng-jun et al., [10] performed the control of a DIPSC and cart system whose boundaries of fuzzy logic membership functions were determined by a genetic algorithm optimization method. The method has been applied in the simulation environment, and it has been observed that the performance of the system has increased. Xiong and Wan [11] proposed the optimal LQR control method for the DIPSC system in numerical simulation. Q and R matrices, which are the weight matrices of the LQR method, were obtained using the particle swarm optimization (PSO) method. Tao et al., [12] proposed an adaptive fuzzy switch swing-up and sliding control method for a DIPSC. The efficacy of the suggested method was demonstrated through simulation studies. In addition, the effect of chatter is significantly reduced in the method.

Adeli et al., [13] modeled a DIPSC, an overhead crane, constructed a Takagi - Sugeno fuzzy model, and designed a parallel distributed fuzzy LQR controller. The method was supported by simulation studies. Hassanzadeh et al. [14] suggested a model-reference adaptive controller approach for the stabilization of a DIPSC and performed it in an experimental setting. In the proposed method, an LQR controller was initially used; however, in the next step, an LQG controller, which combines Kalman-Bucy filter estimation and LQR feedback control, is used to achieve better steady-state performance. LQR and PD control methods have been suggested to stably control a DIPSC [15]. The simulation studies revealed that the PD controller outperforms the LQR controller in terms of performance. Zhang and Zhang [16] proposed the self-adaptive LQR controller method for a planar DIPSC system and applied it in simulation and an experimental environment. According to the results obtained, the authors concluded that the method provides fast response and stability. LQR and LQR-based fuzzy controller design and control in a simulation environment for a DIPSC system were carried out in another study [17]. The LQR-based fuzzy controller has been found to perform better than the LQR method in controlling the DIPSC system, according to the results.

Wang et al. [18] proposed a Pareto-based Multi-Objective Binary Probability Optimization Algorithm (MBPOA)-based LQR controller and this method has been implemented in the DIPSC in simulation and experimental environments. A hybrid type-2 fuzzy logic control method obtained with the help of an RNA genetic algorithm is proposed for the control of a DIPSC. The parameters of Type 1 and Type 2 fuzzy logic methods are optimized by RNA genetic algorithm and compared. Better performance for DIPSC is achieved by using an optimized type-2 fuzzy logic control with RNA genetic algorithm [19]. Sultan and Farej [20] modeled a DIPSC system and simulated it using the LQR control method. According to the simulation results obtained, they saw a 57% and 79% decrease in peak amplitude for the lower arm and upper arm, respectively. Bandari et al., [21] proposed the LQR control method for real-time control of a DIPSC system. The successful demonstration of the controller's ability to restore stability after imparting impact distortion to both the first and second pendulums was made by the testing results.

Banerjee et al., [22] proposed the LQR method for the control of a DIPSC system. The traditional PID method was also used in the study to compare the performance of the method. Simulation of the DIPSC system was performed using the optimal LQR controller method [23]. In this study, the Q and R parameters of the controller are updated, and the G gain matrix is optimized using five different configurations of three different optimization algorithms (Particle Swarm Optimization (PSO), Artificial Bee Colony Algorithm (ABC), and Genetic Algorithm (GA)). Response time and response smoothness were measured for the outcomes produced by each algorithm, both alone and in combination. The controller optimized with the GA algorithm produced the quickest control response, while the

controller optimized with the ABC method had the smoothest response, according to the results.

The results obtained by using each algorithm were evaluated in terms of response speed and response smoothness, in itself and with each other. According to the results, the controller optimized with GA gave the fastest control response, while the smoothest response was provided by the controller optimized with the ABC algorithm. He et al. [24] have conducted a literature study on underdrive robotic systems. The challenges in current research are summarized, and information is provided for future research. Tijani and Jimoh [25] presented a comparative study of a DIPSC system, the optimal control open model predictive control (eMPC), and the linear quadratic control (LQR) method. The open model predictive control (the eMPC) method showed an effective performance compared to the LQR control method, especially in terms of reducing the peak values. Maraslidis et al., [26] proposed a fuzzy logic controller (FLC) for the control of a DIPSC system in a simulation environment. An LQR is used in the article to compare the results of the proposed method. According to the results obtained, it has been seen that the FLC method significantly reduced the stability and peak levels. Gil et al. [27] implemented reinforcement learning-based PD control for a DIPSC in a simulation environment. A DIPSC is simulated using a passive control method based on operator theory [28]. The chaotic dynamics of a DIPSC with a large angle of oscillation are studied based on Hamilton's canonical equation. It is found that the pendulum can maintain the equilibrium state as long as one of the coils has an oscillation angle of 0 degrees [29]. The oscillation and constant-time stabilization control of an incompletely driven DIPSC is carried out in a simulation environment [30].

This study aimed to model and optimally control a double-inverted pendulum system on a cart (DIPSC). A double inverted pendulum system on a cart (DIPSC) was modeled using the Lagrange-Euler method, and classical and optimal LQR control methods were designed for the control of the system. The purpose of the designed controllers is to keep the arms of the double inverted pendulum on the moving cart vertically in balance and to bring the cart to the determined balance position. The Genetic Algorithm (GA), Particle Swarm Optimization (PSO), and Grey Wolf Optimization (GWO) algorithms were used to determine the vitally essential Q and R parameters of the LQR control method, one of the optimal control methods. The DIPSC system was checked using classical LQR and optimal LQR methods. All obtained results are given graphically. The proposed methods are presented and analyzed in tabular form using the settling time and the Mean-Square-Error (MSE) performance criteria. The rest of this article is structured as follows. In Chapter 2, the model of the DIPSC system is presented. Recommended controllers for the system are shown in Chapter 3. GA, PSO, and GWO algorithms are given for the optimization of the parameters of the LQR control method. The simulation results obtained by applying the methods

suggested in Chapter 4 are given numerically and graphically. Chapter 5 summarizes the entire article and provides information on the development of this article and future work.

Modeling of Double Inverted Pendulum System on a Cart (DIPSC) System

Model equations, which have an important place in the control of systems in computer environments, are given below. The DIPSC was modeled using the Lagrange–Euler method. The free-body diagram of the DIPSC system is shown in Figure 1.

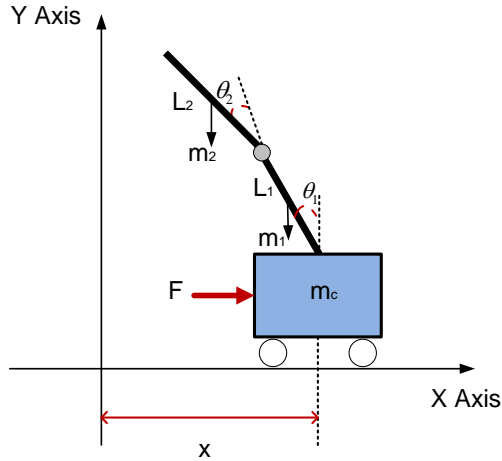


Figure 1. The physical representation of the DIPSC system

In the DIPSC system given in Figure 1, the variable parameters x , θ_1 and θ_2 represent the position of the cart, the angular position of the first pendulum, and the angle position of the second pendulum, respectively. L_1 is the length of the first pendulum, L_2 is the length of the second pendulum, m_c is the mass of the cart, m_1 is the mass of the first pendulum, and m_2 is the mass of the second pendulum. F represents the force acting on the cart. I_1 is the moment of inertia of the first pendulum, and I_2 is the moment of inertia of the second pendulum. The total kinetic and potential energies in the system consist of the kinetic and potential energies of the car and each bar separately. Since the car moves linearly on the horizontal axis, it has a kinetic energy originating from the translational movement only in this axis. Since the rods make both translational and rotational movements, their total kinetic energies constitute the translational and rotational kinetic energy originating from these movements. These Equations are given below.

$$x_{p_1} = x - l_1 \sin \theta_1 \rightarrow \dot{x}_{p_1} = \dot{x} - l_1 \dot{\theta}_1 \cos \theta_1 \quad (1a)$$

$$y_{p_1} = l_1 \cos \theta_1 \rightarrow \dot{y}_{p_1} = -l_1 \dot{\theta}_1 \sin \theta_1 \quad (1b) \quad (12a)$$

$$x_{p_2} = x - l_1 \sin \theta_1 - l_2 \sin (\theta_1 + \theta_2) \quad (2a)$$

$$y_{p_2} = l_1 \cos \theta_1 + l_2 \cos (\theta_1 + \theta_2) \quad (2b)$$

$$\dot{x}_{p_2} = \dot{x} - l_1 \dot{\theta}_1 \cos \theta_1 - l_2 (\dot{\theta}_1 + \dot{\theta}_2) \cos (\theta_1 + \theta_2) \quad (3a)$$

$$\dot{y}_{p_2} = -l_1 \dot{\theta}_1 \sin \theta_1 - l_2 (\dot{\theta}_1 + \dot{\theta}_2) \sin (\theta_1 + \theta_2) \quad (3b)$$

$$T_c = \frac{1}{2} m_c \dot{x}^2 \quad (4)$$

$$T_{p_1} = \frac{1}{2} m_{p_1} (\dot{x} - l_1 \dot{\theta}_1 \sin \theta_1)^2 - \frac{1}{2} m_{p_1} (-l_1 \dot{\theta}_1 \sin \theta_1)^2 + \frac{1}{2} I_p \dot{\theta}_1^2 \quad (5)$$

$$T_{p_2} = \frac{1}{2} m_{p_2} (\dot{x} - l_1 \dot{\theta}_1 \cos \theta_1 - l_2 (\dot{\theta}_1 + \dot{\theta}_2) \cos (\theta_1 + \theta_2))^2 + \frac{1}{2} m_{p_2} (-l_1 \dot{\theta}_1 \sin \theta_1 - l_2 (\dot{\theta}_1 + \dot{\theta}_2) \sin (\theta_1 + \theta_2))^2 + \frac{1}{2} I_p (\dot{\theta}_1 + \dot{\theta}_2)^2 \quad (6)$$

$$V_{p_1} = m_{p_1} g l_1 \cos \theta_1 \quad (7)$$

$$V_{p_2} = m_{p_2} g l_1 \cos \theta_1 + m_{p_2} g l_2 \cos (\theta_1 + \theta_2) \quad (8)$$

The equations of motion of the DIPSC are obtained by taking the following assumptions in the state-space form as follows:

$$\theta_1, \theta_2 \approx 0 \quad (9a)$$

$$\sin \theta_1, \sin \theta_2, \sin (\theta_1 + \theta_2) = 0 \quad (9b)$$

$$\cos \theta_1, \cos \theta_2, \cos (\theta_1 + \theta_2) = 1 \quad (9c)$$

$$\dot{\theta}_1^2, \dot{\theta}_2^2, \dot{\theta}_1 + \dot{\theta}_2^2 = 0 \quad (9d)$$

The equation of motion of a DIPSC is created in the state space model; $\dot{x} = Ax + Bu$ and $y = Cx + Du$ form as follows. The state variables of the DIPSC with trolley are trolley position - velocity and angular position - velocity of each pendulum. The output variables are the car position and the angular position of the pendulums. These variables are given in Equation (10).

$$x = \begin{bmatrix} x_1 \\ x_2 \\ x_3 \\ x_4 \\ x_5 \\ x_6 \end{bmatrix} = \begin{bmatrix} x \\ \theta_1 \\ \theta_2 \\ \dot{x} \\ \dot{\theta}_1 \\ \dot{\theta}_2 \end{bmatrix} \quad y = [x \quad \theta_1 \quad \theta_2] \quad (10)$$

$$\begin{bmatrix} \dot{x}_1 & x_2 \\ \dot{x}_3 & x_4 \\ \dot{x}_5 & x_6 \end{bmatrix} \quad (11)$$

$$A = \begin{bmatrix} 0 & 0 & 0 & 1 & 0 & 0 \\ 0 & 0 & 0 & 0 & 1 & 0 \\ 0 & 0 & 0 & 0 & 0 & 1 \\ 0 & 4.87 & -0.16 & -35.55 & -0.02 & 0.02 \\ 0 & 76.6 & -31.9 & -185.1 & -0.37 & 0.72 \\ 0 & -84.3 & 123.77 & 203.7 & 0.72 & -2.06 \end{bmatrix}$$

$$B = \begin{bmatrix} 0 \\ 0 \\ 0 \\ 4.16 \\ 21.7 \\ -23.89 \end{bmatrix}, \quad C = \begin{bmatrix} 1 & 0 & 0 & 0 & 0 & 0 \\ 0 & 1 & 0 & 0 & 0 & 0 \\ 0 & 0 & 1 & 0 & 0 & 0 \end{bmatrix}, \quad (12b)$$

$$D = \begin{bmatrix} 0 \\ 0 \\ 0 \end{bmatrix} \quad (12c)$$

Controller Design

While designing the controller, it was aimed to keep the arms of the double inverted pendulum with the linear moving cart vertically balanced and to bring the cart in a balanced position. This chapter describes the controller methods designed for the DIPSC. The control of the DIPSC aims to design a controller with minimum error to move the cart so that the actual position of the cart reaches the desired position. The DIPCS was controlled using the Linear Quadratic Regulator (LQR) control method. Here, how parameters of LQR control methods are obtained by using Genetic Algorithm (GA), Particle Swarm Optimization (PSO), and Grey Wolf Optimization (GWO) algorithms are given.

Linear Quadratic Regulator (LQR) Control Design

The Linear Quadratic Regulator (LQR) control method is a modern optimal control method based on state-space representation [32]. LQR is a full-state feedback controller. The primary goal of optimum control is to meet physical constraints to the best possible extent, while at the same time extreme (maximizing or minimizing) an appropriate performance index or cost function. LQR is widely used since it is an optimal and robust control method [33-34]. Below is a performance index for the control strategy that was obtained using state-space equations.

$$J = \frac{1}{2} \int_0^t (x^T(t)Qx + u^T Ru)dt \quad (13)$$

The control system is optimal when the parameters of the performance index are chosen to make the function either minimal or maximal. In classical linear optimal control, the control vector $u(t)$ is chosen so that the performance index is minimized. The performance indicator selected for system control is typically quadratic concerning both $x(t)$ and $u(t)$. It is desired that the integral of the sum of the expression containing Q and R matrices be minimum. This means minimizing Equation 13. Here, Q is a positive semi-definite symmetric matrix, and R is a positive definite number. Q and R are the weight matrices ($Q \geq 0, R > 0$). Then, the linear state feedback rule provides the best control that minimizes J . The control system is optimal when the parameters of the performance index are chosen to make the function either minimal or maximal. The control vector $u(t)$ is chosen in classical linear optimum control so that the performance index is minimized. The performance index chosen for system control is typically quadratic concerning

both $x(t)$ and $u(t)$. The integral of the sum of the expression including the Q and R matrices should be as small as possible. In this case, equation 13 must be reduced. Here, Q is a positive semi-definite symmetric matrix, and R is a positive definite number ($Q \geq 0, R > 0$). Q and R are the weight matrices. Then, the linear state feedback law is given the optimal control that minimizes J .

$$u = -K * x \quad (14)$$

The control strategy in this case aims to reduce the integral of the quadratic performance indicator. The function's value demonstrates how closely the system's real performance matches its intended performance. The given Equation (15) yields the K optimal feedback gain matrix.

$$K = T^{-1}(T^T)^{-1}B^T = R^{-1}B^T P \quad (15)$$

The value of the P positive definite matrix is obtained with the help of Riccati's Equation.

$$A^T P + PA - PBR^{-1}B^T P + Q = 0 \quad (16)$$

In this study, metaheuristic algorithms GA, PSO, and GWO methods were used. These algorithms are frequently used in the literature [35-40]. When using GA, PSO, and GWO to set the Q and R matrices, the first step is to start the chromosome in the GA method, swarm particle in the PSO method, and wolf population in the GWO method. Each chromosome, particle, and wolf population element is represented by a vector n representing the Q and R matrices. $n(1) Q(1,1), n(2) Q(3,3), n(3) Q(5,5)$ and $n(4)$ represent the R -value. Then, parameters such as the population and limits of the algorithms are described. An objective function based on the control input and the Mean Absolute Squared Error is suggested to determine the best control settings. All three algorithms search iteratively until it reaches any of the stopping criteria such as generation or the number of iterations, function tolerance, and time limit to minimize this objective function and find the optimal solution. Figure 2 illustrates the block schema of the LQR control method.

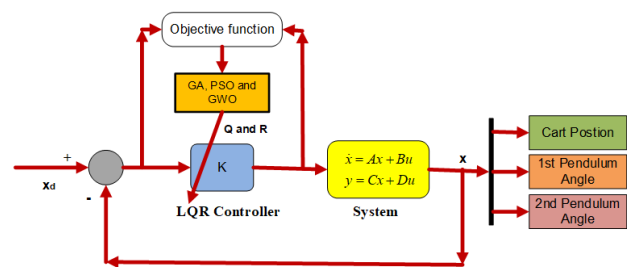


Figure 2. Block diagram of LQR control method

Numerical Results

This chapter provides simulation studies employing a DIPSC's model equations. In the control of the system, optimal LQR control methods were obtained by using classical LQR and GA, and PSO and GWO algorithms were used. The control variables of the system are the position of the cart and the angles of the pendulum. The results were obtained numerically according to the settling time and the MSE criteria, which are the performance criteria of the applied control methods. The physical parameters of

DIPSC were taken as $m_c=1.2$ kg, $m_{p1}=0.097$ kg, $m_{p2}=0.0127$ kg, $L_{p1}=0.2$ m, $l_{p1}=0.16$ m, $L_{p2}=0.34$ m, $l_{p2}=0.18$ m, $b_c=0.001$ Ns/m, and $b_{p1}=b_{p2}=0.024$ Ns/rad. The simulation time was set to 10 seconds. It was obtained from the classical LQR control parameters as $R = [1]$ and $Q = \text{diag} \{43 \ 50 \ 50 \ 11.25 \ 1.50\}$. In all optimization algorithms (GA, PSO, and GWO), the number of populations was taken as 40 and the number of iterations as 100. However, since sufficient convergence could not be achieved with the GA optimization algorithm, the number of populations was taken as 50. In addition, the maximum number of generations in GA was taken as 200, and the crossover and mutation probability as 0.8 and 0.4. The lower and upper limit values for the optimized Q and R parameters are taken as $lb = [1 \ 1 \ 1 \ 0.01]$ and $ub = [1000 \ 1000 \ 1000 \ 100]$. The LQR control parameters obtained using the GA optimization method are $R = [0.021]$ and $Q = \text{diag} \{60.3 \ 0.05 \ 0.03 \ 5.06 \ 0.01\}$. The LQR control parameters obtained using the PSO optimization method are $R = [0.001]$ and $Q = \text{diag} \{100 \ 0.1 \ 0.09 \ 190.6 \ 0.15\}$. The LQR control parameters obtained using the GWO optimization method are $R = [0.1]$ and $Q = \text{diag} \{20 \ 20 \ 600 \ 0 \ 0.15\}$. In Figure 3, a) The linear and angular positions, and b) the error graphs obtained using the classical LQR control method of DIPSC are given.

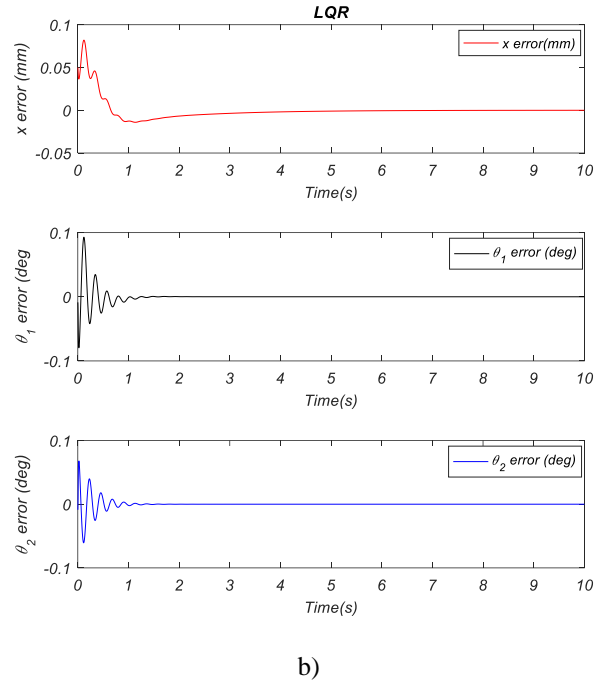
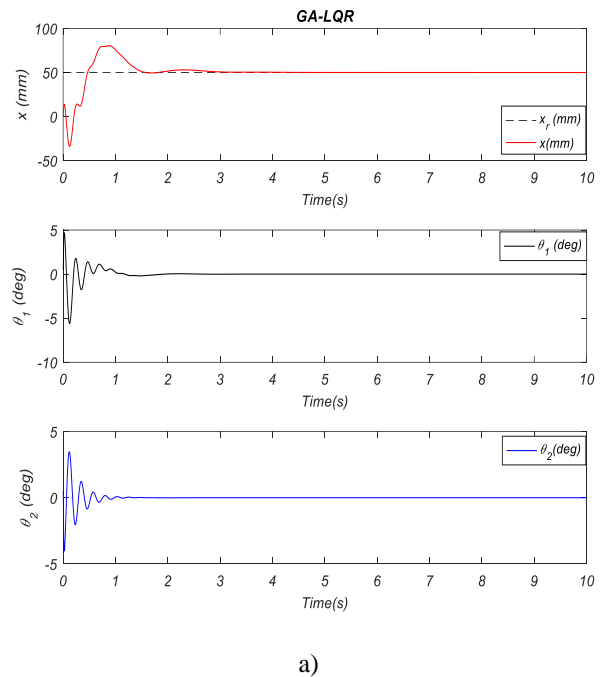
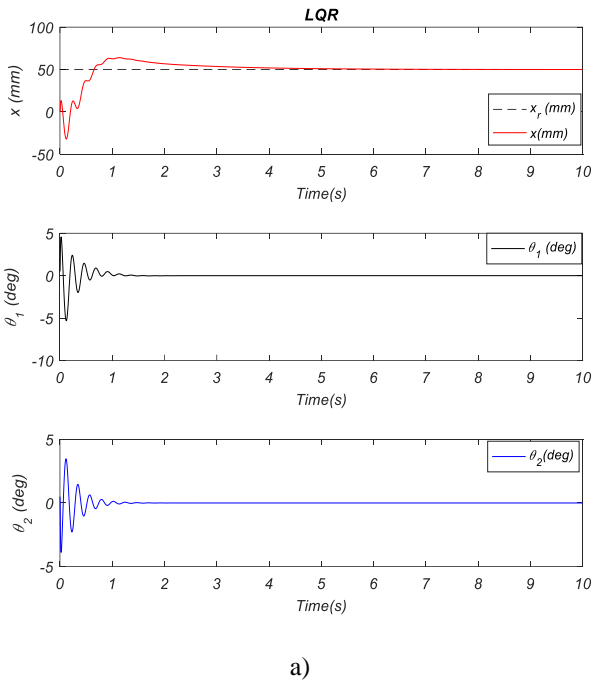


Figure 3. a) The linear and angular positions and b) the error graphs obtained using the classical LQR control method of DIPSC

As shown in Figure 3, the graph obtained as a result of the use of the classical LQR control method shows that the maximum overshoot occurred in the system. It is also seen that the cart reaches a settling time of approximately 5 seconds. In Figure 4, a) linear and angular positions and b) error graphs obtained using the GA-based optimal LQR control method of DIPSC are given.



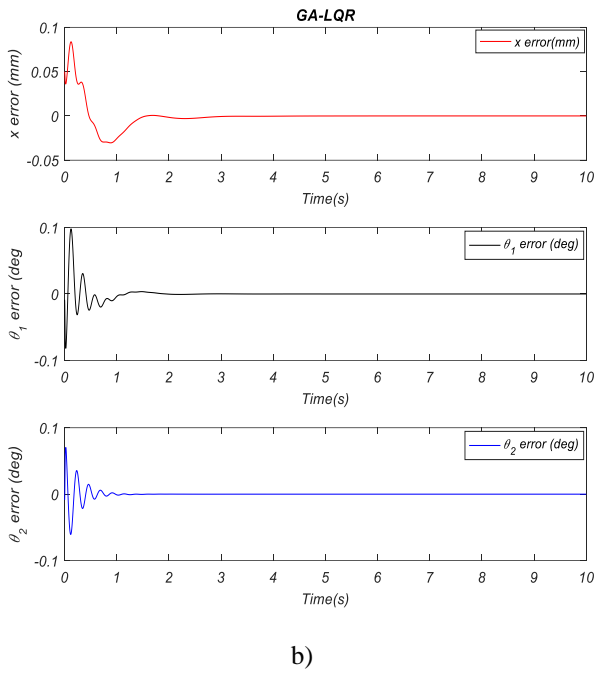


Figure 4. a) The linear and angular positions and b) the error graphs obtained using the GA-based optimal LQR control method of DIPSC

As seen in Figure 4, the graph obtained as a result of the use of the GA-based optimal LQR control method shows that the maximum overshoot in the system is increased compared to the classical LQR method. However, it is seen that the cart reaches a settling time of approximately 4 seconds. In Figure 5, a) linear and angular positions and b) error graphs obtained using the PSO-based optimal LQR control method of DIPSC are given.

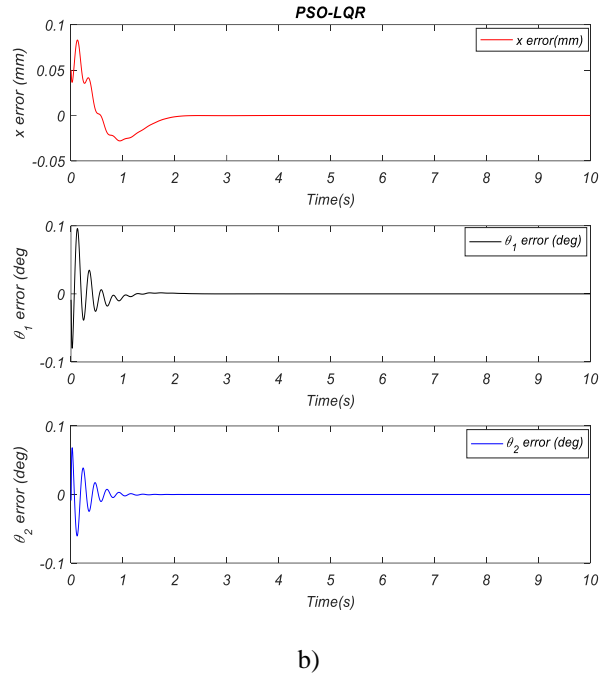
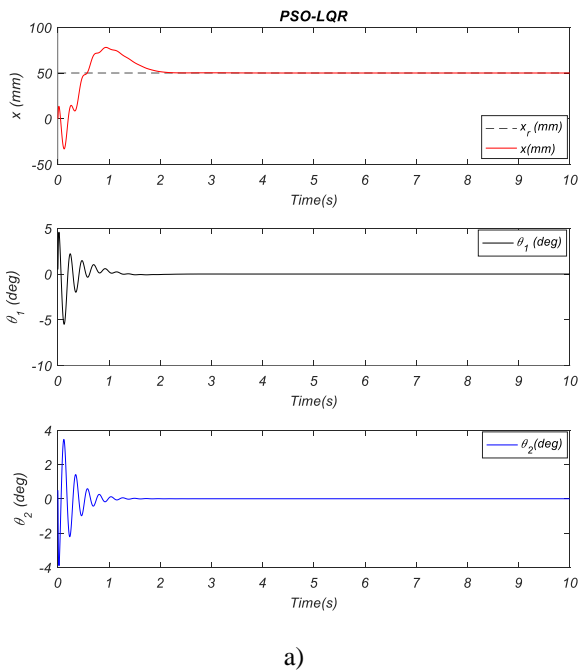
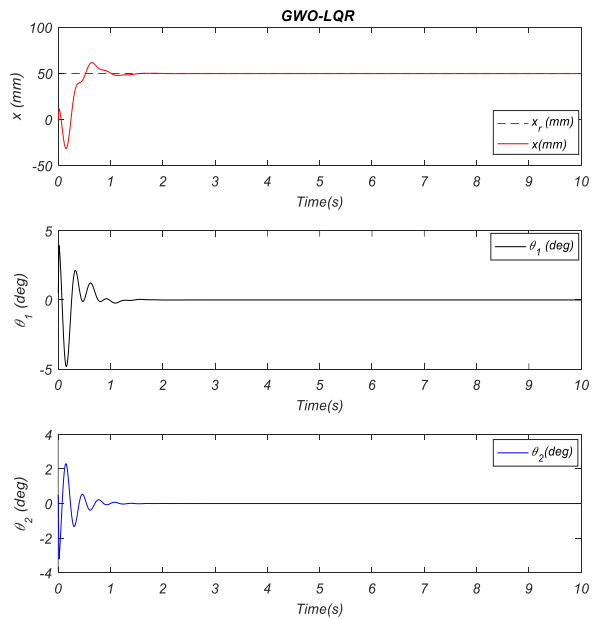


Figure 5. a) The linear and angular positions and b) the error graphs obtained using DIPSC's PSO-based optimal LQR control method

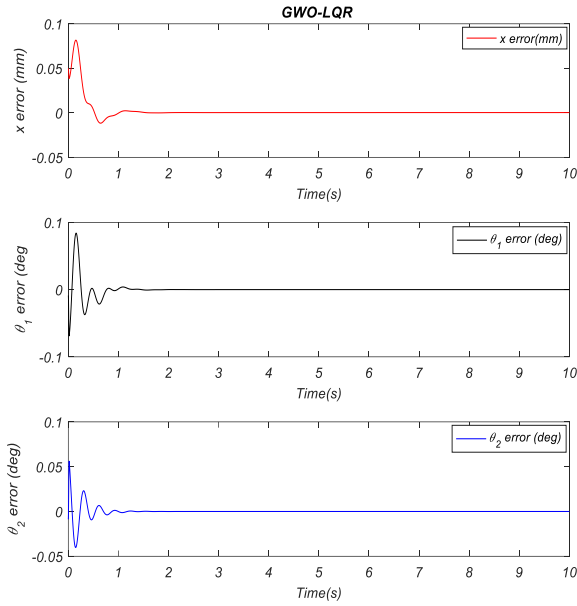
When Figure 5 is examined, it is seen in the graph obtained as a result of the use of the PSO-based optimal LQR control method, that the maximum overshoot in the system decreased slightly compared to the GA-based LQR method, but increased compared to the classical LQR method. However, it is seen that the cart reaches a settling time of approximately 2 seconds. In Figure 6, a) The linear and angular positions and b) error graphs obtained using the GWO-based optimal LQR control method of DIPSC are given.



a)



a)



b)

Figure 6. a) The linear and angular positions and b) the error graphs obtained using DIPSC's GWO-based optimal LQR control method

When Figure 6 is examined, it is seen in the graph obtained as a result of the use of the GWO-based optimal LQR control method that the maximum overshoot occurs in a very small amount in the system and that it is considerably reduced compared to all previous methods. It is seen that the cart reaches a settling time of approximately 1.4 seconds. Figure 7 is given the convergence graph.

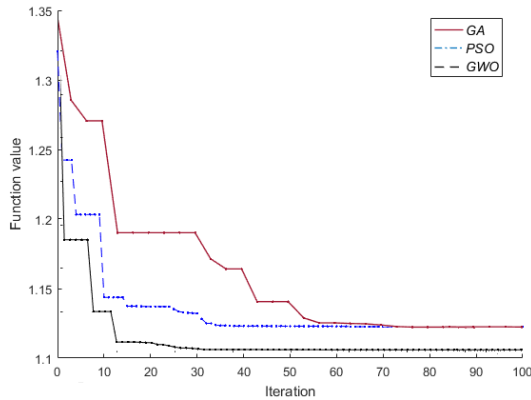


Figure 7. The convergence graph of optimization algorithms

When the convergence graph is examined, it is seen that the best convergence is achieved with the GWO algorithm and this is achieved in approximately 30 iterations. Similarly, it is seen that PSO reaches approximately 40 iterations and GA reaches approximately 75 iterations. Error results will be compared using the performance criteria given below.

$$MSE = \frac{1}{N} \left(\sum_j^N y_{d_j} - y_j \right)^2 \tag{17}$$

If the desired y_{d_j} robot's j . value is y_j then it represents the j . actual value of the robot. y represents the position of the cart or the angular positions of the pendulums. $j=1,2,3,4 \dots N$ is. Tables 1 a and b show the error results obtained by using MSE, which is the performance criterion of classical LQR, GA-based LQR, PSO-based LQR, and GWO-based LQR control methods.

Table 1. The performance comparisons of the linear and angular position tracking error (mm) using a) settling time and b) MSE

a) Settling time

Control type/ Criteria	LQR	GA-LQR	PSO-LQR	GWO-LQR
x	5	4	2	1.4
θ_1	2	2.5	1.8	1.5
θ_2	1.9	1.6	1.4	1.2

b) MSE

Control type/ Criteria	LQR	GA-LQR	PSO-LQR	GWO-LQR
x	$1.82 \cdot 10^{-3}$	$1.65 \cdot 10^{-4}$	$1.52 \cdot 10^{-4}$	$1.41 \cdot 10^{-4}$
θ_1	$1.18 \cdot 10^{-4}$	$2.14 \cdot 10^{-4}$	$9.12 \cdot 10^{-5}$	$9.56 \cdot 10^{-5}$
θ_2	$5.58 \cdot 10^{-5}$	$4.98 \cdot 10^{-5}$	$3.75 \cdot 10^{-5}$	$2.58 \cdot 10^{-5}$

According to the results of the performance error criteria (settling time and MSE-linear/angular position) obtained using the performance criteria in Tables 1a and b, the settling error performance for the classical LQR control method is 5 seconds. The Linear and angular position error values are $1.82 \cdot 10^{-3}$ mm, $1.18 \cdot 10^{-4}$ degrees, and $5.58 \cdot 10^{-5}$ degrees, respectively. According to the performance error criteria given in the table, the settling error performance obtained by using the GA-based LQR control method is 4 seconds. The linear and angular position error values are $1.65 \cdot 10^{-4}$ mm, $2.14 \cdot 10^{-4}$ degrees, and $4.98 \cdot 10^{-5}$ degrees, respectively. According to the performance error criteria given in the table, the settling error performance obtained by using the PSO-based LQR control method is 2 seconds. The linear and angular position error values are $1.52 \cdot 10^{-4}$ mm, $9.12 \cdot 10^{-5}$ degrees, and $3.75 \cdot 10^{-5}$ degrees, respectively. According to the performance error criteria given in the table, the settling error performance obtained by using the GWO-based LQR control method, which is the last method recommended, is 1.4 seconds. The Linear and angular position error values are $1.41 \cdot 10^{-4}$ mm, $9.56 \cdot 10^{-5}$ degrees, and $2.58 \cdot 10^{-5}$ degrees, respectively. Considering all the results obtained, the GWO-based LQR control method outperformed other methods in point of both settling time and MSE error criteria.

Conclusions

In this study, modeling and optimal control of a double-inverted pendulum system on a cart (DIPSC) were performed. The system was modeled using the Lagrange-

Euler method, and classical and optimal Linear Quadratic Regulator (LQR) control methods were utilized for the system's control. The Genetic Algorithm (GA), Particle Swarm Optimization (PSO), and Grey Wolf Optimization (GWO) algorithms were used to determine the vitally essential Q and R parameters of the LQR control method, one of the optimal control methods. The DIPSC system was controlled in the simulation environment by using classical LQR and optimal LQR methods. The results obtained by using the proposed methods the settling time and the Mean-Square-Error (MSE) performance criteria were compared and examined. Considering all the results obtained, the GWO-based LQR control method outperformed other methods in terms of both settling time and MSE error criteria. The physical parameters used in the method are the real parameters of real-time DIPSC systems. It will be of great advantage to use these real parameters during the experimental implementation of the method. In addition, in the simulation environment, the noise in the real environment is added to the control of the system. A 2nd order low pass filter is used to filter this noise. Also, the method can be developed using different optimization techniques and objective functions. In addition, the method can be developed and applications can be made in a real-time laboratory environment.

Ethics Committee Approval

There is no need to obtain permission from the ethics committee for the article prepared.

Conflict of Interest Statement

There is no conflict of interest with any person/institution in the article prepared.

References

- [1] M. McGrath, D. Howard and R. Baker, "The strengths and weaknesses of inverted pendulum models of human walking." *Gait & posture* vol. 41, no. 2, pp. 389-394, 2015.
- [2] Y. Fang, W. E. Dixon, D. M. Dawson and E. Zergeroglu, "Nonlinear coupling control laws for an underactuated overhead crane system." *IEEE/ASME transactions on mechatronics* vol. 8, no. 3, pp. 418-423, 2003.
- [3] X. Huang and C. Chen "Research and Implementation of Self-Balancing Obstacle Vehicle Based On the Principle of Flywheel Inverted Pendulum." *2021 3rd International Conference on Artificial Intelligence and Advanced Manufacture*. 2021, pp. 1070-1073.
- [4] C. He, K. Huang, X. Chen, Y. Zhang and H. Zhao, "Transportation control of cooperative double-wheel inverted pendulum robots adopting Udwadia -control approach." *Nonlinear Dynamics* vol. 91, no. 4, pp. 2789-2802, 2018.
- [5] H. Li, M. Zhihong and W. Jiayin, "Variable universe adaptive fuzzy control on the quadruple inverted pendulum." *Science in China Series E: Technological Sciences* vol. 45, no. 2, pp. 213-224, 2002.
- [6] K. Furuta, T. Okutani and H. Sone, "Computer control of a double inverted pendulum." *Computers & Electrical Engineering* vol. 5. no.1, pp. 67-84, 1978.
- [7] F. Cheng, G. Zhong, Y. Li and Z. Xu, "Fuzzy control of a double-inverted pendulum." *Fuzzy sets and systems* vol. 79, no. 3, pp. 315-321, 1996.
- [8] W. Zhong and H. Rock, "Energy and passivity based control of the double inverted pendulum on a cart." *Proceedings of the 2001 IEEE International Conference on Control Applications (CCA'01) (Cat. No. 01CH37204)*. IEEE, 2001, pp. 896-901.
- [9] A. Bogdanov, "Optimal control of a double inverted pendulum on a cart." *Oregon Health and Science University, Tech. Rep. CSE-04-006, OGI School of Science and Engineering, Beaverton, OR*, 2004.
- [10] D. Cheng-jun, D. Ping, Z. Ming-lu and Z. Yan-fang, "Double inverted pendulum system control strategy based on fuzzy genetic algorithm." *2009 IEEE International Conference on Automation and Logistics*. IEEE, 2009, pp. 1318-1323.
- [11] X. Xiong and Z. Wan, "The simulation of double inverted pendulum control based on particle swarm optimization LQR algorithm." *2010 IEEE International Conference on Software Engineering and Service Sciences*. IEEE, 2010, pp. 253-256.
- [12] C. W. Tao, J. Taur, J. H. Chang and S. F. Su, "Adaptive fuzzy switched swing-up and sliding control for the double-pendulum-and-cart system." *IEEE Transactions on Systems, Man, and Cybernetics, Part B (Cybernetics)* vol. 40, no.1, pp. 241-252, 2009.
- [13] M. Adeli, H. Zarabadipour and M. A. Shoorehdeli, "Anti-swing control of a double-pendulum-type overhead crane using parallel distributed fuzzy LQR controller." *The 2nd International Conference on Control, Instrumentation and Automation*. IEEE, 2011, pp. 401-406.
- [14] I. Hassanzadeh, A., Nejadfard and M. Zadi, "A multivariable adaptive control approach for stabilization of a cart-type double inverted pendulum." *Mathematical Problems in Engineering* 2011 (2011).
- [15] N. Singh and S. K. Yadav, "Comparison of LQR and PD controller for stabilizing Double Inverted Pendulum System." *International Journal of Engineering Research and Development* vol. 1, no. 12, pp. 69-74, 2012.
- [16] J. L. Zhang and W. Zhang, "LQR self-adjusting based control for the planar double inverted pendulum." *Physics Procedia* vol. 24, pp. 1669-1676, 2012.
- [17] N. S. Bhangal, "Design and performance of LQR and LQR based fuzzy controller for double inverted pendulum system." *Journal of Image and Graphics* vol. 1. no. 3, pp. 143-146, 2013.
- [18] L. Wang, H. Ni, W. Zhou, P. M. Pardalos, J. Fang and M. Fei, "MBPOA-based LQR controller and its application to the double-parallel inverted pendulum

- system." *Engineering Applications of Artificial Intelligence* vol. 36, pp. 262-268, 2014.
- [19] Z. Sun, N. Wang, and Y. Bi, "Type-1/type-2 fuzzy logic systems optimization with RNA genetic algorithm for double inverted pendulum." *Applied Mathematical Modelling*, vol. 39, no. (1), pp. 70-85, (2015).
- [20] G. A. Sultan and Z. K. Farej, "Design and Performance Analysis of LQR Controller for Stabilizing Double Inverted Pendulum System." *Circ. Comput. Sci.* vol. 2, no. 9, pp.1-5, 2017.
- [21] N. Bandari, A. Hooshiar, M. Razdan, J. Dargahi and C. Su, "Stabilization of double inverted pendulum on a cart: LQR approach. Su, *International Journal of Mechanical and Production Engineering*, vol. 5, no. 2, 2017.
- [22] R. Banerjee, N. Dey, U. Mondal and B. Hazra, "Stabilization of double link inverted pendulum using LQR." *2018 International Conference on Current Trends towards Converging Technologies (ICCTCT)*. IEEE, 2018, pp. 1-6.
- [23] Ü. Önen, A. Çakan and I. İlhan, "Performance comparison of optimization algorithms in LQR controller design for a nonlinear system." *Turkish Journal of Electrical Engineering and Computer Sciences* vol. 27, no. 3, pp. 1938-1953, 2019.
- [24] B. He, S. Wang and Y. Liu, "Underactuated robotics: a review." *International Journal of Advanced Robotic Systems* vol.16, no.4, 1729881419862164, 2019.
- [25] T. M. Tijani and I. A. Jimoh, "Optimal control of the double inverted pendulum on a cart: A comparative study of explicit MPC and LQR." *Applications of Modelling and Simulation* vol.5, pp. 74-87. 2021.
- [26] G. S. Maraslidis, T. L. Kottas, M. G. Tsiouras and G. F. Fragulis, "Design of a Fuzzy Logic Controller for the Double Pendulum Inverted on a Cart." *Information* vol. 13, no. 8, pp. 379, 2022.
- [27] G. P. Gil, W. Yu and H. Sossa, "Reinforcement learning compensation based PD control for a double inverted pendulum" *IEEE Latin America Transactions*, vol. 17, no. 2, pp. 323-329, 2019.
- [28] N. Bu and X. Wang, "Swing-up design of double inverted pendulum by using passive control method based on operator theory" *International Journal of Advanced Mechatronic Systems*, vol. 10, no. 1, pp. 1-7, 2023.
- [29] J. He, L. Cui, J. Sun, P. Huang and Y. Huang, "Chaotic dynamics analysis of double inverted pendulum with large swing angle based on Hamiltonian function" *Nonlinear Dynamics*, vol. 108, no. 4, pp. 4373-4384, 2022.
- [30] L. Fan, A. Zhang, G. Pan, Y. Du, and J. Qiu, "Swing-up and fixed-time stabilization control of underactuated cart-double pendulum system" *IET Control Theory & Applications*, vol. 17, no. 6, pp. 662-671, 2023.
- [31] B. D. Anderson and J. B. Moore, *Optimal control: linear quadratic methods*. Courier Corporation, 2007.
- [32] T. Abut, "Modeling and optimal control of a DC motor." *Int. J. Eng. Trends Technol* vol. 32, no. 3, pp.146-150, 2016.
- [33] L. M. Argentim, W. C. Rezende, P. E. Santos and R. A. Aguiar, "PID, LQR and LQR-PID on a quadcopter platform." *2013 International Conference on Informatics, Electronics and Vision (ICIEV)*. IEEE, 2013, pp. 1-6.
- [34] S. N. Sivanandam and S. N. Deepa, *Genetic algorithms*. Springer Berlin Heidelberg, 2008, pp. 15-37.
- [35] T. Abut, "Dynamic Model and Optimal Control of A Snake Robot: TAROBOT-1." *International Journal of Scientific & Technology Research* vol. 4, no.11, pp. 4, 2015.
- [36] J. Kennedy and R. Eberhart, "Particle swarm optimization." *Proceedings of ICNN'95-international conference on neural networks*. vol. 4. IEEE, 1995, pp. 1942-1948.
- [37] Y. Shi, "Particle swarm optimization: developments, applications and resources." *Proceedings of the 2001 congress on evolutionary computation (IEEE Cat. No. 01TH8546)*. Vol. 1. IEEE, 2001, vol. 1, pp. 81-86.
- [38] S. Mirjalili, S. M. Mirjalili and A. Lewis, "Grey wolf optimizer." *Advances in engineering software* vol. 69 pp. 46-61, 2014.
- [39] T. Abut and S. Soyguder, "Optimal adaptive computed torque control for haptic-teleoperation system with uncertain dynamics." *Proceedings of the Institution of Mechanical Engineers, Part I: Journal of Systems and Control Engineering* vol. 236, no. 4, pp. 800-817, 2022.
- [40] H. Faris, I. Aljarah, M. A. Al-Betar and S. Mirjalili, "Grey wolf optimizer: a review of recent variants and applications." *Neural computing and applications* vol. 30, 413-435, 2018.